Palaeogeography Palaeoclimatology Palaeoecology
December 2010, Volume 298 Issue 3-4 Pages 311-318
https://doi.org/10.1016/j.palaeo.2010.10.005
https://archimer.ifremer.fr/doc/00230/34135/

Mississippi River discharge over the last similar to 560,000 years - Indications from X-ray fluorescence core-scanning

Kujau Ariane [1, 2, *], Nuernberg Dirk [2], Zielhofer Christoph [3], Bahr Andre [2, 4], Roehl Ursula [5]

[1] Ruhr Univ Bochum, Inst Geol Mineral & Geophys, D-44801 Bochum, Germany.
[2] IfM GEOMAR, Leibniz Inst Meereswissensch, D-24148 Kiel, Germany.
[3] Inst Geog, D-04103 Leipzig, Germany.
[4] Goethe Univ Frankfurt, Inst Geosci, D-60438 Frankfurt, Germany.
[5] Univ Bremen, Marum Ctr Marine Environm Sci, D-28359 Bremen, Germany.

* Corresponding author : Ariane Kujau, email address : Ariane.Kujau@rub.de

Abstract :

The long term history of terrigenous flux to the Gulf of Mexico via the Mississippi River is hardly known. We here present geochemical and sedimentological data to approximate the varying Mississippi River sediment influx into the northeastern Gulf of Mexico (GoM) over the last six glacial-interglacial cycles (MIS 1 to 14). Our study is based on the IMAGES sediment core MD02-2576 that was recovered from the DeSoto Canyon and is located similar to 200 km south to the recent Mississippi River delta and similar to 150 km east of the recent coastline of Florida. Concentrations of siliciclastic elements in bulk sediment samples were estimated from XRF scanning and calibrated by single bulk XRF-analyses. Elemental ratios of the sedimentary record correspond to ratios from the Mississippi River catchment rather than to the core close Alabama and Mobile River catchments. The siliciclastic major element potassium (K) with enhanced surface concentrations in the northwestern Mississippi River catchment shows varying occurrence downcore and here serves as a proxy for Mississippi River sediment discharge variability. Changes in sedimentation rate and magnetic susceptibility further support the variations in Mississippi River influx. Our data were compared with Mississippi River terrestrial archives in the form of loess and terrace deposits that back up our interpretations of enhanced glacial phase Mississippi River influx triggered by strengthened fluvial river runoff and changing fluvial and ice sheet dynamics. Mississippi River influx was at a maximum during glacial MIS 2/3, MIS 8 and MIS 10. Late glacial MIS 6 deviates from this pattern being a period of reduced Mississippi River influx at the core location, probably due to a westward shift of the Mississippi River delta.

Keywords : Mississippi sediment discharge, Mississippi flood dynamics, Gulf of Mexico, Glacial-interglacial cycles, XRF-scanning

1. Introduction

The modern Mississippi River supplies ~ 17,000 m^3/s of freshwater on average per year into the Gulf of Mexico (GoM), with enhanced discharge during the spring month (Wasklewicz et al., 2004). It is responsible for ~66% of the total dissolved organic and inorganic matter transported from the conterminous United States to the ocean (Corbett et al. 2004). The Mississippi River is the main factor in shaping the morphology and hydrography of the coastal northern GoM (Corbett et al. 2004). During the late Pleistocene, the drainage area of the Mississippi River included meltwater from the Laurentide Ice Sheet, from proglacial lakes like Lake Agassiz and the glacial Great Lakes (Tripsanas et al., 2007). However, only little is known about the sediment discharge and composition of the Mississippi River during the past glacial-interglacial cycles and controlling factors. Here, we present Mississippi River sediment discharge proxies in the form of high-resolution geochemical records of the northeastern GoM, which cover the last ~560 kyrs. Our dataset was compared with the variability of terrestrial and marine sediment sources. The newly compiled data are correlated with magnetic susceptibility, reflectivity and $CaCO_3$ data (Nürnberg et al, 2008; Ziegler et al., 2008) as well as element ratios of terrestrial sediment samples (Gustavsson et al., 2001), loess records (Forman and Pierson, 2002), and terrace accumulation phases (Rittenour et al., 2003; 2005) in the Mississippi River catchment area. The core is located in proximity to, but not within, the recent Mississippi River delta, which minimizes direct morphologic processes within the delta region It further ensures that Mississippi River sediment flux is reconstructed that reached the core location.

2. Regional setting

The modern catchment of the Mississippi River covering an area of 3,220,000 km^2 (National Park Service, 2004) lies between the Appalachian Mountains in the east, the southernmost extension of the Great Lakes in the northeast, southernmost Canada in the north and the Rocky Mountains in the west (Fig. 1). The Mississippi River has a length of about 3 705 km (Nipper et al., 2008), with its headwater, Lake Itasca, at 47°N, 95°W in northern Minnesota. It enters the GoM southeast to Baton Rouge, Lousiana, at 29°N, 89°W (Fig. 1). At present, maxima of sediment transport and freshwater

discharge are relatively synchronous, occurring during February to May (Bianchi et al., 2007). About 50% of the sediment discharge flows to the west and ~50% to the east and south (Corbett et al., 2004; Gordon and Goni, 2004). Most of the suspended load is deposited within 30 km off the delta and is remobilized and dispersed throughout a much larger area in particular during the winter months by winds and waves (Corbett et al., 2006).

The northwestern continental slope of the GoM shows a disturbed morphology (Tripsanas et al., 2007) and a cumulative occurrence of salt diapirs (Bouma et al., 1996), whereas the DeSoto Canyon area in the northeastern GoM shows undisturbed layering (ODP seismic line 126, Joyce et al., 1990). The modern sea floor surface lithology of the northeastern GoM between the Mississippi River delta and Cape San Blas (Florida) is dominated by terrigenous sediments mainly provided by the Mississippi River (c.f. Gordon and Goni, 2004; Corbett et al., 2006). East and south of Cape San Blas carbonate ooze is the dominating sediment while close to the shore quartz sand is prevailing (Balsam and Payne Beeson, 2003).

3. Material and Methods

The IMAGES sediment core MD02-2576 (29°00.09'N, 87°07.14'W) was retrieved in 2002 during cruise MD-127 with RV *Marion Dufresne* and has a length of 45.77 m. Core MD02-2576 is located next to the 34 m long core MD02-2575 (29°00.10'N, 87°07.13'W) (c.f. Nürnberg et al, 2008; Ziegler et al., 2008) and close to ODP Site 625 (Joyce et al., 1993) and core GS7109-2 (Emiliani, 1975). Sediment core MD02-2576 was retrieved from the eastern margin of the DeSoto Canyon in the northeastern GoM with predominantly terrigenous surface sediments (Nipper et al., 2008). The distance between the core location and the Mississippi River delta is~200 km.

The age model of core MD02-2576 was constructed by correlation of the reflectivity record (L* = the fraction in % of incident radiation reflected by a surface, depending on colour) with that of MD02-2575. The reliable age scale of core MD02-2575 was constructed using high resolution benthic $\delta^{18}O$ stratigraphy and AMS^{14}C-dating in the younger part (Nürnberg et al., 2008). For the

period not covered by MD02-2575, the L* record of MD02-2576 was correlated to the global LR04 benthic foraminiferal $\delta^{18}O$ stack (Lisiecki and Raymo, 2005) (Fig. 2). The first 40 cm of core MD02-2576 show core disturbance in the form of compressed sediment leading to a younger age to depth-correlation, probably caused by the core retrieval procedure that puts enhanced pressure on the core top segment (Nürnberg et al., 2008). Sedimentation rates (in cm kyr-1) were calculated by dividing the thickness of sediment intervals between age control points by their duration of deposition. Sedimentation rates of terrigenous matter is calculated according to:

$$\text{sed. Rate}_{\text{terr.}} = \text{sed. rate}_{\text{bulk}} * (\text{siliciclastics \% / 100}) \qquad (1)$$

Geochemical element ratios of samples from the different catchment areas are useful tools to gain information about the sediment provenance of fluvial sediments (Amorosi et al., 2002; Moldenhauer et al., 2008). Core MD02-2576 was analyzed with the Avaatech XRF Core Scanner (ACS) at University Bremen for the intensities of the major elements Ti, Fe, K, Ca and Sr. These elements were measured non-destructively and directly at the split sediment surface every cm for 30 seconds at an X-ray current of 0.087 mA and 20 kV ... (c.f. Tjallingii et al., 2007). As shown by Tjallingii et al. (2007), the observed elements remain relatively unaffected by changing physical properties, i.e. water content. The element intensities in counts per second (cps) acquired with the XRF Core Scanner can be converted into quantitative data in weight percent (wt.% or ppm) and parts per million (ppm) by calibration with bulk-XRF analysis. For this purpose, 16 samples were selected at significant minima, maxima and changeover points indicated by the XRF-scan records (see Fig. 6). The absolute element concentrations were determined with a Philips PW 2400 bulk-XRF spectrometer at IFM-GEOMAR.

For Ti, Fe, Ca, and Sr, the correlation coefficients r^2 between XRF-scanner data (cps) and bulk-XRF measurements (wt% or ppm) are 0.65, 0.69, 0.80, and 0.68, respectively. For K, the correlation is much weaker (r^2=0.36), due to the fact that the K peak in the XRF intensity spectrum is attached to

the Ca peak and is easily tampered by a varying Ca signal. We therefore normalised K in counts per second to total counts in order. to receive an independent K signal and to improve correlation (r^2=0.68):

$$K_{corrected}=K_{counts\ per\ second}/\text{total counts} \quad (2)$$

All K values given in the following are calculated based on the corrected K counts.

4. Results and Discussion

Sedimentation on the western Florida Shelf is dominated by foraminifer/coccolith ooze (Blake and Doyle, 1983), leading to $CaCO_3$ concentrations of >40% during interglacials (Nürnberg et al., 2008). The terrigenous portion is mainly restricted to the silt and clay fractions, and is known to originate from heterogeneous sources (Goni et al., 1997; Gordon and Goni, 2003). Based on the chemical differences in the source areas, ratios Fe/Ti, K/Ti, and K/Fe were used to characterize the source of the terrigenous matter in our downcore record. For core MD02-2576, we observe a good correlation between Ti and Fe (r^2=0.88), suggesting that these elements share a common terrigenous source. In this respect, dilution processes are considered unimportant, as K is not affected equally (r^2=0.56 for Ti versus K, Fig. 3). Although Fe is commonly prone to diagenetic remobilization in pore waters, we expect no diagenetic alteration of the Fe record. The good correlation of Fe to Ti, which is largely inert to diagenetic processes (c.f. Richter et al., 2006), and the similarity of their downcore records imply that the sediment core is not affected by diagenetic processes. The major element K is deviating from the other siliciclastic elements. The low correlation of K to Ti (r^2=0.56) and Fe (r^2=0.52) points to a different terrigenous source for K.

The irregular surface elemental concentrations throughout the United States (Gustavsson et al., 2001, Fig. 4) support our notion: Ti occurs with high concentrations in the southern and eastern part of the MR catchment and partly, in the Alabama and Mobile River catchments, which are the continental areas closest to the core location. The remaining areas exhibit rather low concentrations (Fig. 4). Fe

is distributed uniformly at medium concentrations. High concentrations are recognized only in the northeast, while lowest concentrations are observed in the Alabama/Mobile River catchments (Fig. 4). The distribution pattern of K, in contrast, is clearly differentiated with highest concentrations in the Mississippi River catchment area and with lowest concentrations in the Alabama/Mobile River catchments close to the core site (Fig. 4) In Fig. 5, ratios of the siliciclastic major elements Ti, Fe and K of both the modern Mississippi River catchment and the adjacent Alabama/Mobile catchment, taken from the element distribution charts of Gustavsson et al. (2001) by setting grid points (see Fig. 4), are compared to those of core MD02-2576 (see Table 1). As the downcore elemental ratios plot within the field of the Mississippi River catchment and are quite different from the Alabama/Mobile catchment, the Mississippi catchment as major source for the MD02-2576 sediment is further constrained.

The calculated bulk sedimentation rate for MD02-2576 matches the sedimentation rate for the terrigenous fraction (Fig. 6) suggesting that the main portion of sediment is contributed by terrigenous flux rather than by marine productivity. Most notably, sedimentation rates are enhanced during MIS 2, 3 and 8 pointing to significantly enhanced accumulation of Mississippi River sediments.

The magnetic susceptibility record of core MD02-2575 closely resembles the terrigenous (carbonate free fraction) flux to the core location (Nürnberg et al., 2008) (Fig. 6). Downcore variations of the terrigenous fraction closely correspond to the terrestrial element group Ti, Fe and K, which originate mainly from clay minerals, feldspars and heavy minerals. The Ca-record closely resembles the $CaCO_3$ percentages and is anticorrelated to the terrestrial element records, implying that terrestrial element variations may be diluted by $CaCO_3$. $CaCO_3$ is mainly derived from calcareous skeletons of marine foraminifera and pteropods, whose abundances vary on glacial-interglacial scales with marine productivity enhanced during interglacial times (Nürnberg et al., 2008). Lowered $CaCO_3$ concentrations during glacial phases (~20% during MIS 2, 3, and 8 c.f. Fig. 6), instead result from

both, a strengthened flux of terrigenous material towards the site location, and a significantly reduced marine productivity.

To account for temporal changes in $CaCO_3$ production, the terrigenous elements (Ti and K) were normalized to Ca (Fig. 6). Pure elemental downcore records as shown in Fig. 6 appear rather similar, both more directly reflect variations of terrestrial sediment input as shown by the close correlation to terrestrial archives on Mississippi River sediment transport (see below). The terrigenous elements are enhanced during glacial MIS while Ca is low. Vice versa, they are low during interglacial phases when Ca is enriched. The element K partly deviates from this pattern, in particular during MIS 3/4, 6, 7 and 12 (c.f. Fig. 6). Taking further into account the spatial surface K differentiation across the United States with high K concentrations in the Mississippi catchment and low K values in the Alabama/Mobile area (Fig. 4), we use the downcore K-variations as unique indication for changes in Mississippi River sediment flux towards the core location.

Enhanced K concentrations in core MD02-2576 point to strengthened fluvial sediment supply from the western Mississippi River catchment area, as it the prominent source of K-enriched sediments. The suspension load being distributed from the river mouth across the northern GoM most likely causes the enhanced sedimentation rates at the core location. Gravitational downslope transport of shelf and upper continental slope sediments is rather unlikely, as turbiditic sequences are not observed in the core and the seismic profile (ODP seismic line 126, ODP Site 625; Joyce et al., 1990).

Both, the fact that 50% of the discharged Mississippi River sediment load is transported southward and eastward and the proposed dispersal of Mississippi-derived sediment by wave action over a wide area (Corbett at al., 2004; Gordon and Goni, 2004), especially during the winter month (Corbett et al., 2006), supports our notion of a Mississippi River dominated depositional environment at the DeSoto Canyon core location. At present, both the maximum freshwater discharge and the maximum sediment supply of the Mississippi River occur from February to May (Bianchi et al.,

2007). Supposedly, this pattern of synchronous maxima holds true for past glacial phases as well. Both, sedimentation rates and magnetic susceptibilities show high similarity to the K signal (Fig. 6), which are all representing Mississippi River discharge. It supports our interpretation of maximum Mississippi River input during glacial phases, most pronounced during MIS 2, 8, 10, and 12.

Glacial sea-level drops and shelf exposure significantly reduced the distance between the core location and, therefore, affected the terrigenous sediment flux at core MD02-2576 (Winn et al., 1995). Most likely, the spatially variable progradation of the Mississippi River mouth across the shelf during sea level low stands (Womack, 2006) was highly effective in shaping the sedimentation pattern on the shelf and across the continental slope. This might have been especially important for glacial MIS 6, as neither maxima in K nor in magnetic susceptibility and sedimentation rate at core MD02-2576 point to enhanced Mississippi River discharge. The Ti-values remain relatively high, rather indicating the background continental runoff apart from Mississippi River contribution (Fig. 6).

Relative variations between K and Ti indicated by K/Ti ratios enable to differentiate between Mississippi River and Alabama/Mobile sediment supply. As K reflects sediment contribution from the Mississippi River catchment while Ti is indicative of terrigenous matter provided by continental runoff, low K/Ti ratios most likely denote the relative predominance of the “background” terrigenous supply. An enhanced relative contribution from the Mississippi River to the core location, instead, is indicated by maxima in the K/Ti record. The downcore K/Ti ratios are well above 4.5, which is significantly higher than the K/Ti ratios from the Alabama/Mobile region (~1.6; see Tab. 1), but definitely lower than the K/Ti ratios from the Mississippi River catchment (~6-10). The initially high K/Ti ratio close to the Mississippi River mouth is apparently diluted on the eastward transport of Mississippi River sediments as Ti from continental runoff is added, but remains definitely higher than the K/Ti ratio characteristic for the Alabama/Mobile catchment.

Hence, Mississippi River sediment supply dominated sediment accumulation at core MD02-2576 over the last 570 kyrs. During interglacial sea level high stands, when sedimentation rates were

commonly low at DeSoto Canyon, the Mississippi River contribution still exceeds the terrigenous flux from continental runoff, indicated by high K/Ti ratios (Fig. 7). In particular during late MIS 2 and 12, and during MIS 6, however, exceptionally low K/Ti ratios occur during times of relative sea level low stands This points to relative high continental runoff indicated by high Ti values, while the relative importance of Mississippi River sediment supply is diminishing as K is low.

At the neighbouring site MD02-2575, Nürnberg et al. (2008) already reported on reduced coarse carbonate and magnetic susceptibility values during MIS 6 as well as on high sea surface salinities atypical for full glacial times. This can be explained by a significantly diminished impact of Mississippi River discharge on the northeastern GoM hydrography. A westward shift of the Mississippi River delta as indicated by Tripsanas et al. (2007, c.f. Fig. 1) during MIS 6 probably caused fluvial sediment supply mainly directed towards the northwestern GOM, and less freshwater dispersal into the northeastern GOM.

Lateral migration of the Mississippi River mouth system is indeed crucial for sediment dispersal across the northern GOM. However, it certainly cannot account solely for all the different glacial sedimentation patterns observed at core MD02-2576. In particular, the less pronounced maxima seen during glacial MIS 12 may be attributed to less intense glacial conditions, different routing of meltwater, and/or a changing location of the river mouth.

While glaciers covered the northern Mississippi River catchment during full glacial times, the Mississippi River drained proglacial lakes resulting in an enlarged Mississippi River drainage area compared to the recent Mississippi River catchment (Rittenour et al., 2003; 2005; Tripsanas et al., 2007). The widened drainage area, documented for the late Pleistocene and presupposed also for the previous cold phases, led to enhanced Mississippi River sediment discharge into the GoM as reflected in the K record of core MD02-2576. The southward expansion of the Laurentide Ice Sheet is known to have enhanced the Mississippi River sediment discharge into the GoM during the last glacial phase (Tripsanas et al., 2007), also by blocking of passages for continental runoff to the Atlantic and Pacific oceans. Additionally, seasonal melting at the ice sheet margins may have

provided intensified water supply (Marshall and Clarke, 1999). Prominent Mississippi River sediment discharge up to five times higher during glacial conditions than at present interglacial conditions was already assumed by Emiliani (c.f. Gunter, 1976). However, megafloods due to outbursts from Lake Agassiz (Teller et al., 2002; Teller, 2007) are not detectable in our record.

The lower Mississippi River floodplain was in a braiding regime during glacial MIS 2 and 4 between ~20-60 ka (Rittenour et al., 2005; Wasklevicz et al., 2004) (Fig. 8) and probably also during earlier glacial phases. While meandering is an indication for low to mid-energy fluvial environments under constant climatic conditions (Gray and Harding, 2007), braiding is a typical glacial process of periglacial areas (Zepp, 2004) and results in high-energy and highly variable flow conditions (Nanson and Croke, 1992). Glacial activity in the headwaters of the Mississippi River probably set free enhanced meltwater pulses in winter to spring with high amounts of sediment load (Gray and Harding, 2007). Permafrost and less dense vegetation cover during glacial phases reduced the water storage capacity and hence, strengthened surface run-off in the Mississippi River area (Meckler et al., 2008). The loess accumulation phases of the Mississippi River valley (Fig. 8, Forman and Pearson, 2006) indicate less dense vegetation and larger availability of erodible material. Loess is the dominant surficial deposit within the drainage area of the Mississippi river (Follmer, 1996), and periods of loess deposition in North America are associated with strengthened meltwater and sediment delivery (Forman and Pierson, 2002). Mississippi River floodplain aggradation phases (see Rittenour et al., 2003; 2005) also imply enhanced Mississippi River sediment supply and coincide with main phases of sediment accumulation at core MD02-2576 during MIS 2/3/4 (~ 60-20 ka; Fig. 8).

5. Conclusions

The temporal Mississippi River sediment discharge was deduced from marine sediment core MD02-2576 for the last ~560 kyrs. The potassium proxy record mainly reflects fluvial sediment influx, as supported by the sedimentation rate, magnetic susceptibility data and backed up by terrestrial

archives. Main sedimentation phases identified in these terrestrial archives coincide with phases of significantly enhanced Mississippi River discharge from the marine archive. Climatic changes, leading to waxing and waning of the Laurentide ice-sheet, precipitation changes over N-America, sea level fluctuations, and – closely related –Mississippi River delta shifting probably caused the Mississippi River discharge variability. Our study points to prominent Mississippi River sediment input during glacial MIS 2/3, late 8 and 10. The extremely reduced Mississippi River signal during MIS 6 is related to a shift of the Mississippi River delta to the west.

Acknowledgements

We would like to thank T. Westerhold and V. Lükies of MARUM, University Bremen, Germany, for the support during the XRF measurements as well as D. Rau of IfM-GEOMAR, Kiel, Germany, for the bulk-XRF measurements and R. Tjallingii of NIOZ, Texel, The Netherlands, for helpful discussions. We acknowledge the constructive remarks of F. Lamy and one anonymous reviewer.

Appendix A. Supplementary data

Supplementary data associated with this article can be found, in the online version, in Elsevier Web products, including ScienceDirect.

References

Amorosi, A., Centineo, C.M., Dinelli, E., Lucchini, F., Tateo, F., 2002. Geochemical and mineralogical variations as indicators of provenance changes in Late Quaternary deposits of SE Po Plain. Sedimentary Geology 151, 273–292.

Balsam, W.L., and Payne Beeson, J., 2003. Sea-floor sediment distribution in the Gulf of Mexico. Deep-Sea Research 1 (50), 1412-1444.

Bianchi, T.S., Galler, J.J., Allison, M.A., 2007. Hydrodynamic sorting and transport of terrestrially derived organic carbon in sediments of the Mississippi and Atchafalaya Rivers. Estuarine, Coastal and Shelf Science 73, 211-222.

Blake, N.J. and Doyle, L.J., 1983. Infaunal-sediment relationships at the shelf-slope break. In: The Shelfbreak: Critical Interface on Continental Margins. D.J. Stanley and G.T: Moore. SEPM Special Publications 33, 381-389.

Bouma, A.H., Coleman, J.M., Meyer, A.W., 1996. Initial Reports Deep Sea Drilling Project, Washington (U.S. Government Printing Office)

Corbett, R.D., McKee, B., Duncan, D., 2004. An evaluation of mobile mud dynamics in the Mississippi River deltaic region. Marine Geology 209, 91-112.

Corbett, R.D., McKee, B., Allison, M., 2006. Nature of decadal-scale sediment accumulation on the western shelf of the Mississippi River delta. Continental Shelf Research 26, 2125-2140.

Emiliani, C., Gartner, S., Lidz, B., Elridge, K., Elvey, D.K., Huang, T.C., Stipp, J.J., Swanson, M.F., 1975. Paleoclimatological analysis of Late Quaternary cores from northeastern Gulf of Mexico. Science 26, 1083-1089.

Follmer, L.R., 1996. Loess studies in central United States: Evolution of concepts. Engineering Geology 45 (1-4), 287-304.

Forman, S., and Pierson, J., 2002. Late Pleistocene luminescence chronology of loess deposition in the Missouri and Mississippi river valleys, United States. Paleoceanography, Paleoclimatology, Paleoecology 186, 25-46.

Gordon, E.S., and Goni, M.A., 2004. Controls on the distribution and accumulation of terrigenous organic matter in sediments from the Mississippi and Atchafalaya river margin. Marine Chemistry 92, 331-352.

Gray, D., and Harding, J.S, 2007. Braided river ecology. A literature review of physical habitats and aquatic invertebrate communities. New Zealand Department of Conservation. Science for Conservation 279.

Gunter, G., 1979. The annual Flows of the Mississippi River. Gulf Research Reports 6 (3), 283-290.

Gustavsson, N., Bolviken, B., Smith, D.B., Severson, R.C., 2001. Geochemical landscapes of the conterminous United States – New map presentations for 22 elements. U.S. Geological Survey, 1-36.

Joyce, J.E., Tjalsma, R.C., Prutzman, J.M., 1990. High-resolution planktonic stable isotope record and spectral analysis for the last 5.35 m.y.: Oceanic Drilling program site 625 northeast Gulf of Mexico. Paleoceanography 5 (4), 507-529.

Köster, E.A., 2005. The Physical Geography of Western Europe. Oxford University Press 41, Oxford.

Kraus, R.T. and Secor, D. H., 2004. Incorporation of strontium into otoliths of an estuarine fish. Journal of Experimental Marine Biology and Ecology 302, 85-106.

Laskar, J., 1990. The Chaotic Motion of the Solar System: A Numerical Estimate of the Size of the Chaotic Zones. Icarus 88, 266-291.

Lisiecki, L.E., and Raymo, M.E., 2005. A Pliocene-Pleistocene stack of 57 globally distributed benthic $\delta^{18}O$ records. Paleoceanography 20, doi: 10.1029/2004PA001071.

Marshall, S.J., Clarke, G.K.C., 1999. Modeling North Atlantic freshwater runoff through the last glacial cycle. Quaternary Research 52, 300-315.

Meckler, A.N.M., Schubert, C.J., Hochuli, P.A., Plessen, B., Birgel, D., Flower, B.P., Hinrichs, K.-U., Haug, G.H., 2008. Glacial to Holocene terrigenous organic matter input to sediments from Orca Basin, Gulf of Mexico – A combined optical and biomarker approach. Earth and Planetary Science Letters 272 (1-2), 251-263.

Miller, K.G., Kominz, M.A., Browning, J.V., Wright, J.D., Mountain, G.S., Katz, M.E., Sugarman, P.J., Cramer, B.S., Christie-Blick, N., Pekar, S.F., 2005. The Phanerozoic record of global sea-level change. Science 310 (5752), 1293-1298.

Moldenhauer, K.-M., Zielhofer, C., Faust, D., 2008. Heavy metals as indicators for Holocene sediment provenance in a semi-arid Mediterranean catchment in northern Tunisia. Quaternary International 189, 129-134.

Nanson GC, Croke JC., 1992. A genetic classification of floodplains. Geomorphology 4: 459-486.

National Park Service U.S. Department of the Interior. 2004. "General Information about the Mississippi River", Mississippi River and Recreation Area. www.nps.gov

Nipper, M., Sánchez Chávez, J.A., Tunnell Jr., J.W., 2008. GulfBase : Resource Database for Gulf of Mexico Research. World Wide Web electronic publication. http://www.gulfbase.org, 14.April 2008.

Nürnberg, D., Ziegler, M., Karas, C., Schmidt, M.W., Tiedemann, R., 2008. Interacting Loop Current variability and Mississippi River discharge over the past 400 kyrs. Earth and Planetary Science Letters 272, 278-289.

Richter, T.O, van der Gaast, B., Vaars, A., Gieles, R., de Stigter, H., de Haas, H., van Weering, T.C.E., 2006. The Avaatech XRF Core Scanner: technical description and applications to NE Atlantic sediments. In: New Techniques in Sediment Core Analyses. The Geological Society of London, Special Publications 267, 39-50.

Rittenour, T.M., Goble, R.J., Blum, M.D., 2003. An optical age chronology of Late Pleistocene fluvial deposits in the northern lower Mississippi valley. Quaternary Science Reviews 22, 1105-1110.

Rittenour, T.M., Goble, R.J., Blum, M.D., 2005. Development of an OSL chronology for Late Pleistocene channel belts in the lower Mississippi valley, USA. Quaternary Science Reviews 24, 2539-2554.

Röhl, U., Brinkhuis, H., Stickley, C., Fuller, M., Schellenberg, St., A., 2004. Sea Level and Astronomically induced environmental changes in Middle and Late Eocene sediments from the East Tasman Plateau. In: The Cenozoic Southern Ocean: Tectonics, Sedimentation and Climate Change between Australia and Antarctica. Geophysical Monograph Series 151, 127-151.

Teller, J.T., Leverington, D.W., Mann, J.D., 2002. Freshwater outbursts to the oceans from glacial Lake Agassiz and their role in climate change during the last deglaciation. Quaternary Science Reviews 21, 879-887.

Teller, J.T. 2007. North American late-Quaternary meltwater and floods to the oceans: Evidence and impact – Introduction. Palaeogeography, Palaeoclimatology, Palaeoecology 246, 1-7.

Tjallingii, R., Röhl, U., Kölling, M., Bickert, T., 2007. Influence of the water content on X-ray fluorescence core-scanning measurements in soft marine sediments. Geochemistry, Geophysics, Geosystems 8 (2).

Tripsanas, E.K., Bryant, W.R., Slowley, N.C., Bouma, A.H., Karageorgis, A.P., Berti, D., 2007. Sedimentological history of Bryant Canyon area, northwest Gulf of Mexico, during the last 135 kyr (Marine Isotope Stages 1-6): A proxy record of Mississippi River discharge. Paleoceanography, Paleoclimatology, Paleoecology 246, 137-161.

Wasklevicz, T.A., Anderson, S., Liu, P.-S., 2004. Geomorphic context of channel locational probabilities along the Lower Mississippi River, USA. Geomorphology 63, 145-158.

Wiley, J., and Sons, 1999. The Mississippi Drainage Basin, USA. http://geographyalltheway.com/ib_geography/ib_drainage_basins/imagesetc/mississippi_drainage_basin700.jpg

Winn Jr., R.D., Roberts, H.H., Kohl, B., Fillon, R.H., Bouma, A.H., Constans, R.E., 1995. Latest Quaternary deposition on the outer shelf, northern Gulf of Mexico: Facies and sequence stratigraphy from Main Pass Block 303 shallow core. Geological Society of America Bulletin 107, 851-866.

Zepp, H., 2004. Geomorphologie. Ferdinand Schöningh Verlag, Paderborn, 3rd edition.

Ziegler, M., Nürnberg, D., Karas, C., Tiedemann, R., Lourens, L.J., 2008. Persistent summer expansion of the Atlantic Warm Pool during glacial abrupt cold events. NatureGeosciences 277, 601-605.

Figure captions

Fig. 1. Map of North America with the shape of the recent Mississippi River catchment (bold black line, according to Wiley, 1999) and areas of terrestrial archives used for comparison (black squares): terrace deposits (Rittenour et al., 2005) and loess records (Forman and Pierson, 2002). Sediment core MD02-2576 (29°00.09'N, 87°07.14'W) (this study) and adjacent core MD02-2575 (29°00.10'N 87°07.13'W) (Nürnberg et al., 2008; Ziegler et al., 2008) in the northeastern Gulf of Mexico indicated by a black circle. The recent Mississippi River (MR) delta and delta location during Marine Isotopic Stage (MIS) 6 (Tripsanas et al., 2007) are shown as black squares; the location of Cape San Blas, Florida (29°67.00'N, 85°37.00'W), discussed in the text, shown as black dot (chart from esrimap, U.S. Geological Survey).

Fig. 2. Chronostratigraphy of IMAGES core MD02-2576 from DeSoto Canyon over the last 560 kyrs. The stratigraphic framework of MD02-2576 is based on tuning the L* record (a) (this study, red) to the L* record of adjacent core MD02-2575 (b) (Nürnberg et al., 2008). The stratigraphy of MD02-2575 is based on AMS^{14}C-dating and tuning the foraminiferal (*Uvigerina peregrina*) δ^{18}O record (c) (Nürnberg et al., 2008, blue) to the global benthic reference stack LR04 (d) (Lisicki and Raymo, 2005, brown). The filtered 22 kyr and 41 kyr components of the benthic δ^{18}O record of MD02-2575 are in accordance to precession and obliquity solutions (Laskar, 1990), supporting the validity of the age model. The depth/age relationship suggests continous and uniform sedimentation over the past 560 kyrs. Marine Isotopic Stages (MIS) are given in red lettering (c.f., Köster, 2005; Lisiecki and Raymo, 2005).

Fig. 3. Terrigenous elements within MD02-2576. We observe good correlation between Fe [wt.%] and Ti [wt%] ($r^2 = 0.88$), and a weaker correlation between K [wt.%] and Fe [wt.%] ($r^2 = 0.52$), and K [wt.%] and Ti [wt.%] ($r^2 = 0.56$).

Fig. 4. Distribution of surface element concentrations across North America from Gustavsson et al. (2001): Fe (upper image), Ti (middle image), and K (lower image). The modern Mississippi River catchment area is delineated by the green line, the Alabama/Mobile River catchment is in red. Blue colours indicate low, yellow medium and red colours high element concentrations. The K-distribution map shows position of grid-points used for balancing the geochemical composition of different catchment areas (c.f. Table 1).

Fig. 5. Terrigenous mass element ratios of core MD02-2576 (core data = orange circles) in comparison to those of surface sediments from the Mississippi River catchment (green rectangles, c.f. green framed area Fig. 4) and the Alabama/Mobile catchments (red circles, c.f. red framed area Fig. 4). The maximum K/Fe value from the Mississippi River catchment gridpoint (K = 2.12 to Fe = 1, c.f. Table 1) is not shown.

Fig. 6. Geochemical parameters of core MD02-2576 (covering ~560 kyr) in comparison to sedimentological parameters of core MD02-2575 (covering ~400 kryr). Dashed line boxes indicate phases of main deviation of K from Ti. a) Ca (red); b) $CaCO_3$ = total inorganic carbon*8.333 (violet) (Nürnberg et al., 2008); c) Ti (green); d) Ti/Ca (light green); e) K (blue); f) K/Ca (light blues); g) siliciclastics% (= 100%-$CaCO_3$%, terrigenous material as total organic carbon percentages are on average <0.5% (unpublished data), biogenic opal was not detected, turquoise); h) magnetic susceptibility (black) of core MD02-2575 (Nürnberg et al., 2008); i) bulk sedimentation rate (grey) and terrigenous sedimentation rate (purple). Bulk sedimentation rates range between ~0.4 cm/kyr and ~36.7 cm/kyr, the terrigenous sedimentation rates range between ~0.2 cm/kyr and ~30.6 cm/kyr. Element concentrations, initially measured in counts per second by the XRF-scanner and calibrated by single bulk XRF-measurements, are given in wt%; grey bars indicate interglacial MIS (according to Lisicki and Raymo, 2005, and Köster, 2005); stippled areas indicate phases of main deviation of K from Ti and Fe. Black arrows indicate depth levels, where single bulk XRF-measurements were carried out to calibrate the XRF-scans.

Fig. 7. Relative proportion of Mississippi River sediment supply (approximated by K concentrations) versus continental runoff (approximated by Ti concentrations) reaching the core location as K/Ti (green; 5 kyr-steps smoothed), in deviation from the Holocene mean value (0-10 ka) in comparison to changes in sea-level (black; Miller et al., 2005). High K/Ti ratios imply a relative predominance of sediment supplied via the MR compared to continental runoff. Grey bars indicate interglacial MIS.

Fig. 8. a) Phases of loess deposition in the Mississippi valley (Forman and Pierson, 2006; black dots with error bars); b) appearance of lower Mississippi terrace levels in meters above sea level (asl; horizontal lines for orientation), and phase of river braiding (Rittenour et al., 2005, boxes and grey horizontal bar, respectively); c) K of core MD02-2576 over the last ~120 ka; d) Magnetic susceptibility (Mag. sus.) of core MD02-2575 (Nürnberg et al., 2008); e) terrigenous sedimentation rate of core MD02-2576. Light blue bars indicate major sedimentation phases seen both in terrestrial (loess deposits from Forman and Pierson, 2006 and Lower Mississippi terrace levels, see Fig. 1) and marine (MD02-2575/76) archives. Grey bars indicateinterglacial MIS.

Table 1 Surface element concentrations for Ti, Fe, and K for the Mississippi River and the Alabama/Mobile River catchments (bold type), according to the grid-points set for this study. Numbers (italic, bold type) from 1 to 15 in the upper line denote the west-east position of grid-points. Numbers from 1 to 12 in the left column denote the north-south position of grid-points (c.f. Fig. 4 lower right).

Table 1

Titanium in %	***1***	***2***	***3***	***4***	***5***	***6***	***7***	***8***	***9***	***10***	***11***	***12***	***13***	***14***	***15***
1	0.21	0.21	0.21												
2	0.27	0.21	0.23	0.23	0.23	0.27	0.23	0.25	0.25						
3	0.21	0.21	0.17	0.23	0.23	0.27	0.27	0.29	0.27	0.56	0.37				
4		0.17	0.17	0.25	0.23	0.23	0.27	0.23	0.19	0.19	0.34	0.15	0.15		
5			0.15	0.25	0.17	0.19	0.21	0.21	0.19	0.23	0.19	0.15	0.23		0.47
6			0.27	0.18	0.17	0.17	0.25	0.25	0.29	0.29	0.29	0.27	0.27	0.47	0.51
7			0.27	0.21	0.19	0.27	0.29	0.29	0.29	0.29	0.29	0.47	0.56	0.47	0.47
8				0.18	0.25	0.27	0.29	0.44	0.37	0.37	0.51	0.6	0.65	0.56	0.56
9				0.18	0.23	0.21	0.29	0.32	0.32			**0.6**	0.44	0.47	0.56
10					0.25	0.27	0.23	0.23	0.37			**0.56**	**0.44**	**0.44**	**0.37**
11												**0.56**	**0.44**	**0.37**	**0.44**
12												**0.34**	**0.34**	**0.21**	**0.37**
Iron in %															
1	2.3	3.2	2.3												
2	3.2	2.3	3.2	2.3	2.3	2.3	2.3	2.3	3.2						
3	2.3	2.3	2.3	2.3	2.3	2.3	2.3	2.3	2.3	2.3	1.6				
4		2.3	2.3	2.3	2.3	2.3	2.3	2.3	2.3	1	1.6	1	1.1		
5			2.3	2.3	1.2	1.3	2.3	2.3	2.3	1.4	1.2	1.9	2.3		2.3
6			2.3	2.3	2.3	2.3	1.9	2.3	3.2	2.3	2.3	2.3	3.2	3.2	3.8
7			2.3	1.8	1.9	2.3	2.3	2.3	1.9	1.9	1.9	2.3	3.5	3.2	2.3
8				1.9	1.9	1.9	2.3	2.3	1.9	1.3	2.6	2.3	3.2	3.2	3.8
9				1.9	1.9	1.3	1.2	1.4	2.1			**2.3**	2.3	3.5	5.1
10					1.3	1.9	1.2	3.2	2.3			**1.6**	**2.3**	**2.3**	**1.9**
11												**1.1**	**1.3**	**1**	**1**
12												**1**	**1**	**1**	**1**
Potassium in %															
1	1.94	1.94	1.94												
2	1.94	1.94	1.94	1.94	1.94	1.62	1.62	1.23	1.35						
3	1.94	1.94	1.94	1.94	1.94	1.62	1.62	1.23	1.35	2.12	2.54				
4		1.94	2.12	1.94	1.43	1.94	1.62	1.23	1.23	2.12	2.54	1.23	1.23		
5			2.12	2.12	1.77	2.12	1.94	1.23	1.23	1.62	1.62	1.23	1.23		1.23
6			2.12	2.32	2.32	2.12	2.12	1.23	1.35	1.48	1.62	1.62	1.94	1.23	1.23
7			2.78	2.32	2.32	2.12	1.94	1.43	1.35	1.35	1.62	1.62	1.94	1.23	1.23
8				2.12	2.32	2.12	1.94	1.23	1.23	1.35	1.23	1.23	0.86	1.94	1.94
9				1.94	1.94	2.12	0.86	0.6	0.86			**1.23**	1.23	1.35	0.55
10					1.94	1.62	0.94	0.6	0.6			**0.6**	**0.86**	**1.23**	**0.55**
11												**0.55**	**0.55**	**0.55**	**0.55**
12												**0.55**	**0.55**	**0.55**	**0.55**

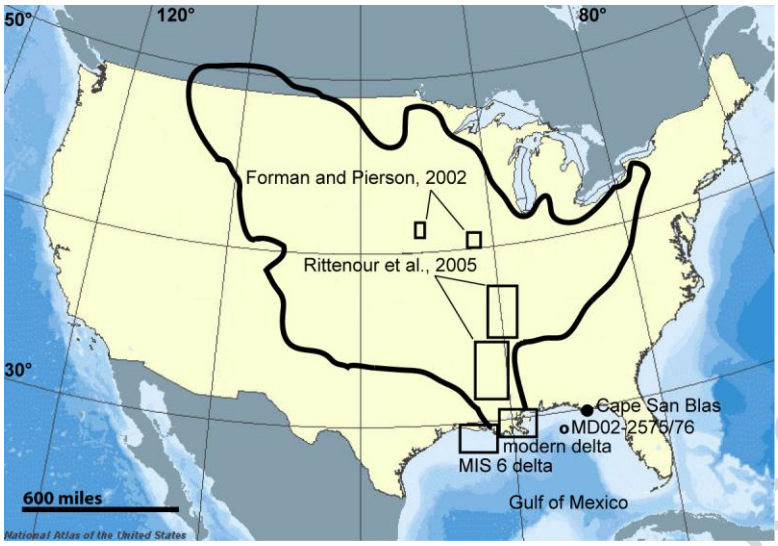

Figure 1

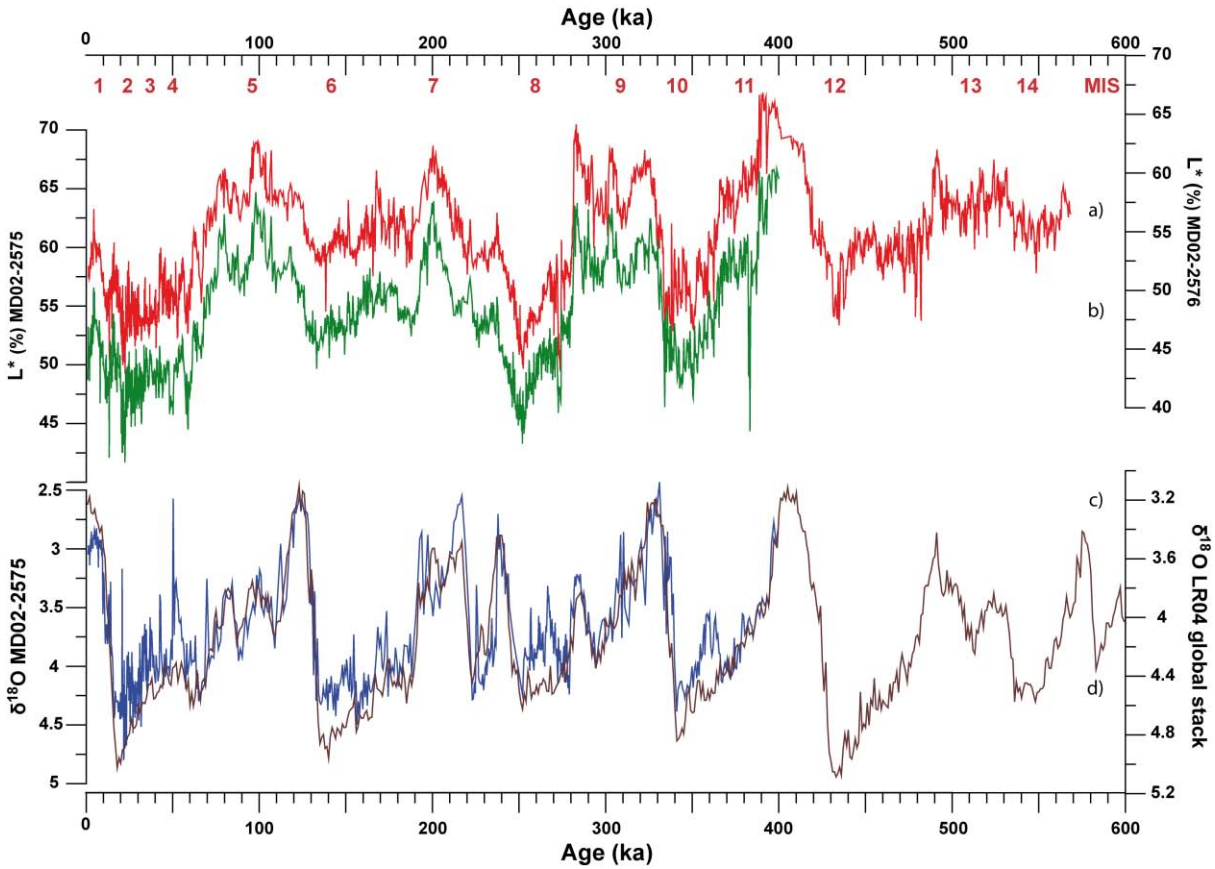

Figure 2

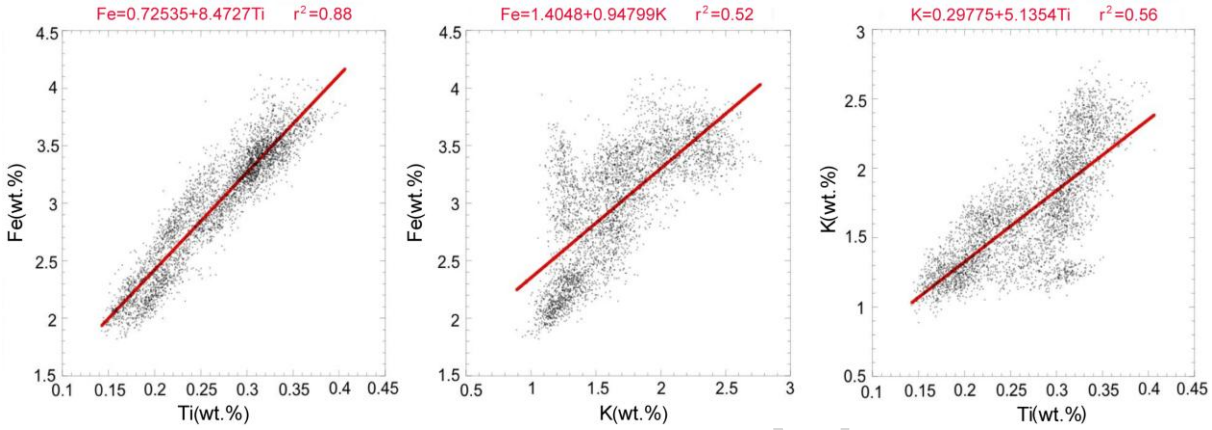

Figure 3

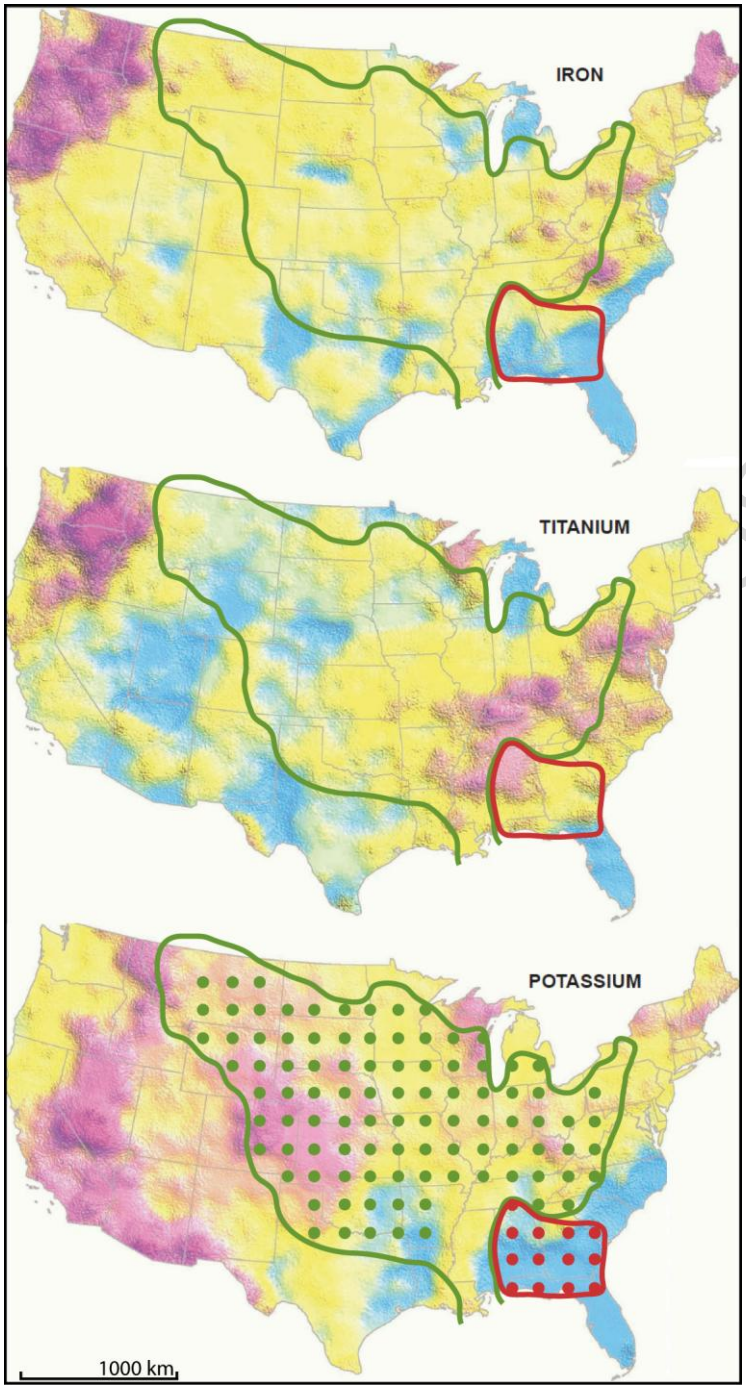

Figure 4

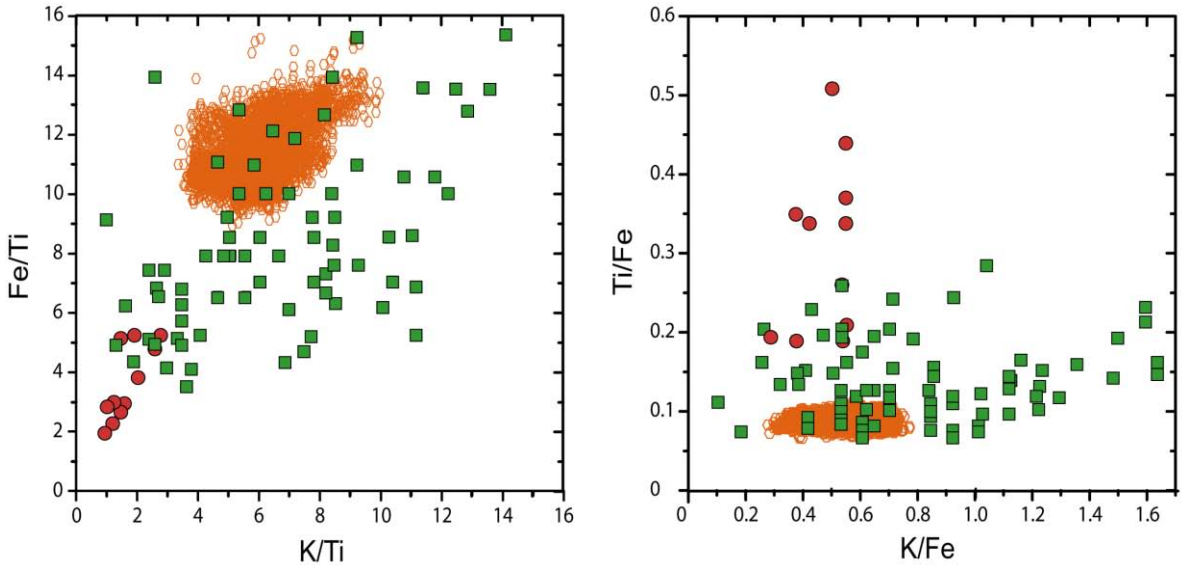

Figure 5

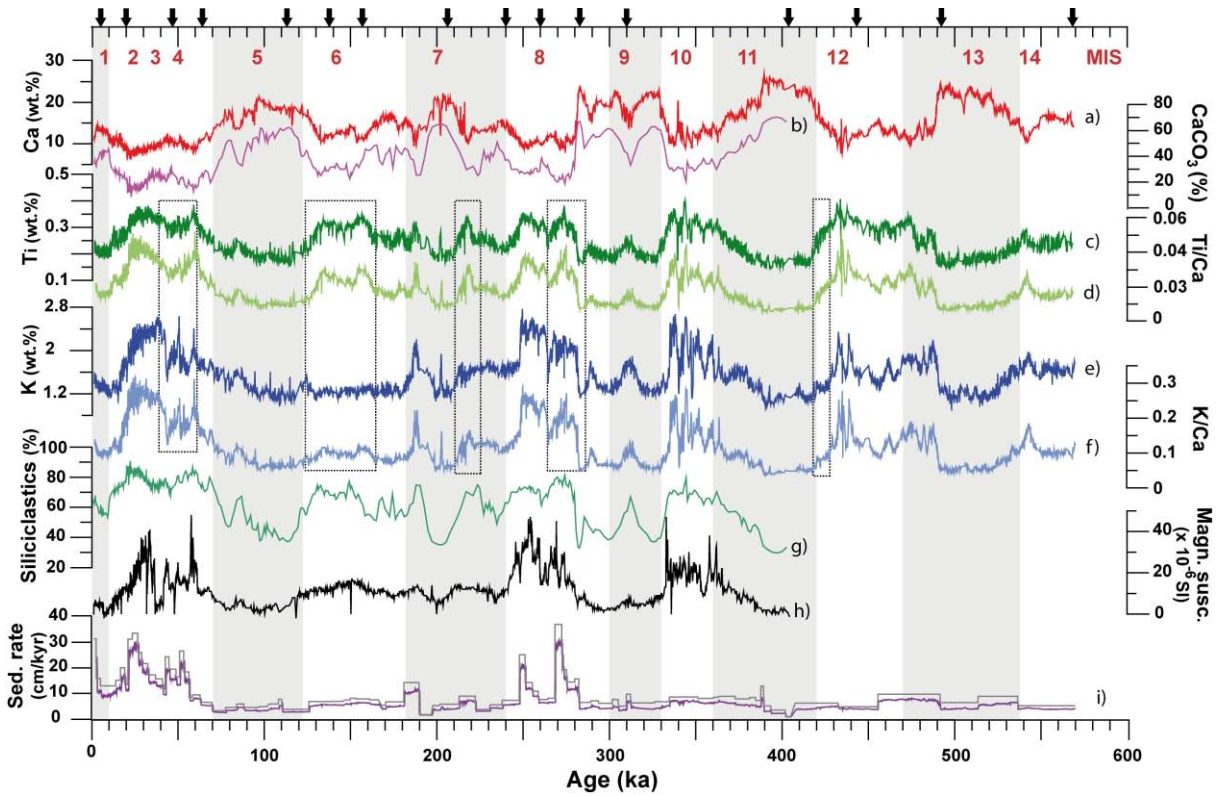

Figure 6

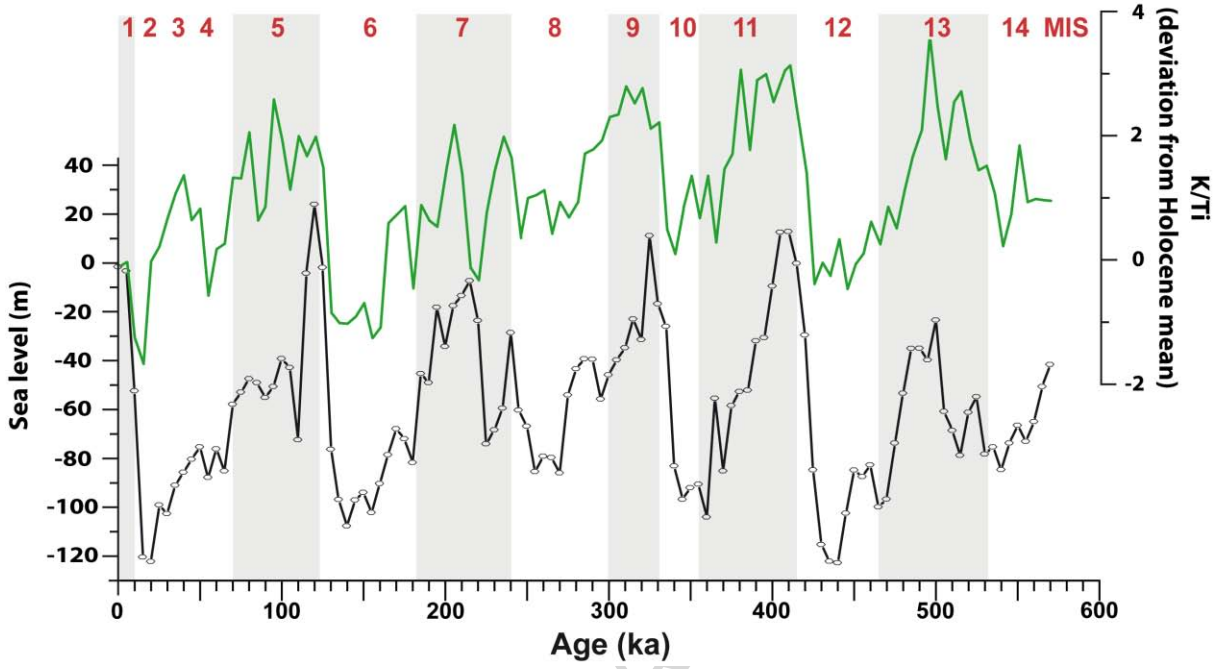

Figure 7

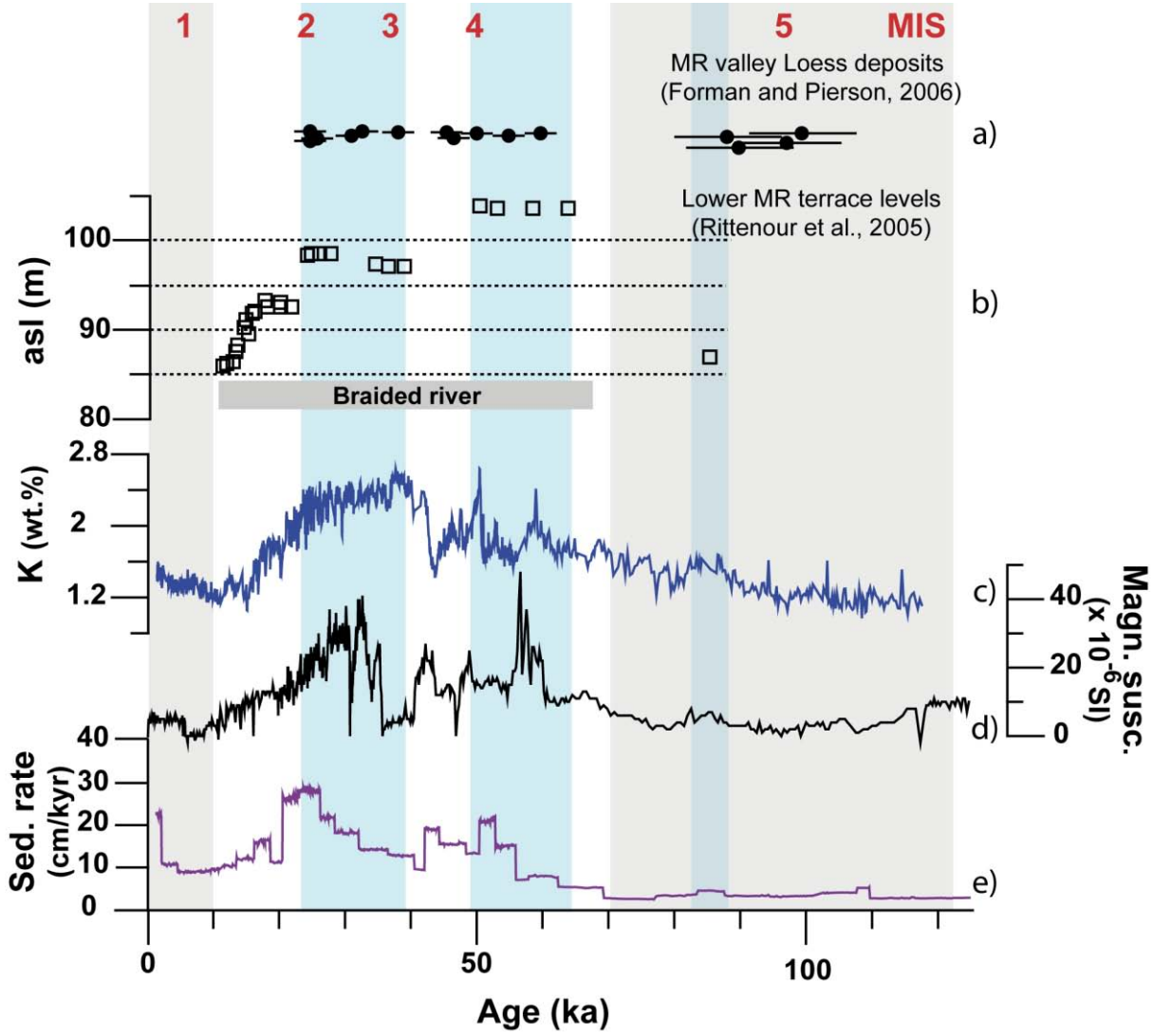
1
2
3
4
5
MIS
MR valley Loess deposits
(Forman and Pierson, 2006)
a)
Lower MR terrace levels
(Rittenour et al., 2005)
asl (m)
100
90
80
b)
Braided river
K (wt.%)
2.8
2
1.2
c)
Magn. susc.
(x 10-6 SI)
40
20
0
d)
Sed. rate
(cm/kyr)
40
30
20
10
0
e)
0
50
100
Age (ka)

Figure 8